International Journal of Technical Innovation in Modern Engineering & Science (IJTIMES)
Impact Factor: 5.22 (SJIF-2017), e-ISSN: 2455-2585
Volume 5, Issue 05, May-2019

THERMAL RADIATION, HEAT SOURCES, HALL CURRENTS ON CONVECTIVE HEAT AND MASS TRANSFER ANALYSIS ON PERISTALTIC FLOW OF WILLIAMSON FLUID IN A SYMMETRIC CHANNEL UNDER INCLINED MAGNETIC FIELD

S.Sridhar [1], V. Ramesh Babu [2]

[1] *Research Scholar, Rayalaseema University, Kurnool, A.P. India*
[2] *Department of Mathematics, Rashtriya Sanskrit Vidyapeetha, Central Deemed University, Tirupati, A.P., India*

Abstract:

We investigate the Hall Effect on the peristaltic flow of Williamson fluid in presence of convective heat and mass transfer condition under inclined magnetic field. Thermal radiation, heat source and Soret effects are included in this analysis. Solutions for stream function, velocity, temperature and concentration are obtained here under the long wavelength and low Reynolds number assumptions. The effects of different parameters on the axial velocity (u), temperature (θ), concentration (C), pressure drop (Δp), frictional force (F), rate of heat and mass transfer (Nu&Sh) and the pumping characteristics are discussed through graphs.

Keywords: Thermal Radiation, Heat Source, Hall Current, Williamson Fluid, Magnetic Field

INTRODUCTION

In Non-Newtonian fluids, the most commonly encountered fluids are pseudo- plastic fluids. The study of the boundary layer flow of pseudo-plastic fluids is of great interest due to its wide range of application in industry such as extrusion of polymer sheets, emulsion coated sheets like photographic films, solutions and melts of high molecular weight polymers, etc.

The diverse characteristics of Non-Newtonian fluids lead to various constitutive equations in the literature The Navier Stokes equations alone are insufficient to explain the rheological properties of fluids. Therefore, rheological models have been proposed to overcome this deficiency. To explain the behaviour of pseudo-plastic fluids many models have been proposed like the power law model, Carreaus model, Cross model and Ellis model, but little attention has been paid to the Williamson fluid model. Williamson [35] discussed the flow of pseudo-plastic materials and proposed a model equation to describe the flow of pseudo-plastic fluids and experimentally verified the results. Lyubimov and Perminov [15] discussed the flow of a thin layer of a Williamson fluid over an inclined surface in the presence of a gravitational field. Dapra and Scarpi [4] developed the perturbation solution for a Williamson fluid injected into a rock fracture.

In certain problems of conductive physiological fluids, the study of magneto-hydrodynamic (MHD) peristaltic flow of a fluid is of special interest. In fact, the influence of magnetic field may be utilized as a blood pump in carrying out cardiac operations for the flow of blood in arteries with arterial disease like arterial stenosis or arteriosclerosis. The usage of the giant magneto-resistive technology which is a device that applies a magnetic field with a very sensitive sensor, accurately detecting the small movements of an object within a magnetic field. This technology has the potential to facilitate the study of peristaltic activity in some tubular structures such as bowel, fallopian tube and perhaps even in the *vas deferens*. Hence peristalsis of MHD Eyring–Powell fluid in a channel is discussed by Noreen and Qasim [21]. Mekheimer *et al.* [16] observed the effects of magnetic field and space porosity on compressed Maxwell fluid. Effects of nanofluid and inclined magnetic field on peristaltic transport of fluid are discussed by Akram [1]. Ravikumar [25] investigated the peristaltic flow of a couple stress fluid through magnetic field at low Reynolds number in a flexible channel. Peristaltic flow of MHD Jeffrey fluid through finite length cylindrical tube is investigated by Tripathi *et al.* [31]. Rashidi *et al.* [22, 23, 24] analyzed the steady and unsteady MHD flows over rotating disks by considering different assumptions such as thermo-diffusion and diffusion-thermo effects, entropy generation and optimization of entropy generation as well. B′eg *et al.* [3] discussed the magneto-bio-rheological model of micropolar fluid in porous medium and obtained the solution by using homotopy analysis method. Ellahi [5] discussed the MHD and temperature-dependent viscosity in pipe flow of a non-Newtonian fluid. Sheikholeslami *et al.* [27] observed the MHD effects in Cu-water nanofluid. Another important aspect in MHD is related to Hall Effect.

Vajravelu et al [32] have discussed the Peristaltic transport of a Williamson fluid in asymmetric channels with permeable walls. Navaneeswara Reddy et al [20] have analysed the effect of partial Slip on peristaltic motion of a Williamson fluid through a porous medium in a planar channel. Jyothi et al [12] have investigated the Slip effects on MHD peristaltic transport of a Williamson fluid through a porous medium in a symmetric channel. Hunaira Yasmin et al [11] have discussed peristaltic flow of an incompressible and electrically conducting Williamson fluid in a symmetric planar channel with heat and mass transfer, Hall effects, viscous dissipation and Joule heating are also taken into account. Veerakrishna et al [33] have discussed the peristaltic flow of an incompressible, electrically conducting Williamson fluid in a symmetric planar channel through a porous medium with heat and mass transfer under the influence of inclined magnetic field of an inclinationα. Hall effects, viscous dissipation and joule heating are considered. Verakrishna et al [34] have analysed the peristaltic MHD flow of an incompressible and electrically conducting Williamson fluid in a symmetric planar channel with heat and mass transfer under the effect of inclined magnetic field.

Sulochana [30] analysed the peristaltic MHD flow of an incompressible, electreically conducting, Williamson fluid in a symmetric planar channel through a porous medium with heat and mass transfer under the influence of inclined magnetic field. Sarada et al [26] have presented the effects of partial slip and convective boundary condition on magnewtohydrodynamic mixed convection flow in the presence and absence of joule heating. Khalid et al [13] have investigated the influence of magnetic field on peristaltic flow of an incompressible Williamson fluid in a symmetric channel with heat and mass transfer with convective boundary conditions. Naheeda Iftikar et al [19] have analysed convective heat transfer with radially magnetic field of an incompressible Williamson fluid with peristaltic motion and joule heating in a curved channel.

The Williamson fluid is a material that falls into the category of viscoelastic shear thinning fluids. It represents the behaviour of pseudo-plastic materials whose apparent viscosity or consistency decreases instantaneously with an increase in shear rate [2, 8, 16]. Also it can be noted that transfer of energy/mass for flowing fluids does not only take place through simple conduction/diffusion, instead, bulk motion of the fluid also plays an important role in the transfer phenomenon. Bulk motion of the fluid can produce considerable alteration in the results of transfer phenomena.

FORMULATION OF THE PROBLEM:

We analyse the peristaltic transport of an incompressible, electrically conducting Williamson fluid in a vertical symmetric channel through a porous medium with heat and mass transfer and under the influence 0f inclined magnetic field of an angle of inclination α as shown in the figure.1. Hall effects are taken into account. The basic equations governing the flow, heat and mass transfer flow of an electrically conducting Williamson fluid v through a porous medium in the presence of heat sources and thermo diffusion are

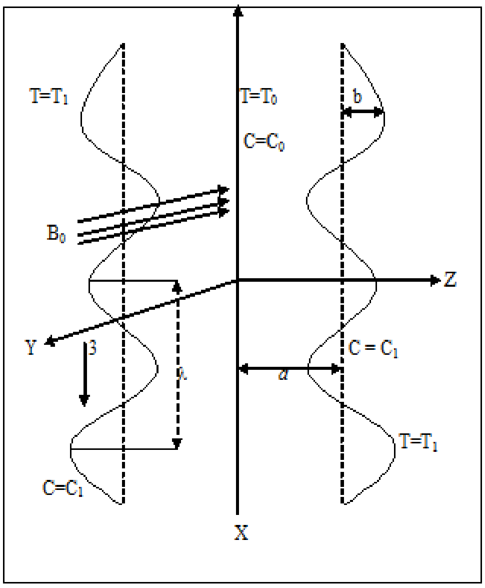

Fig.1: Physical Configuration of the Problem

The continuity equation:

$$\nabla.\overline{V} = 0 \qquad (2.1)$$

Momentum equation

$$\rho \frac{d\overline{V}}{dt} = -\nabla p + \nabla.\overline{S} + \vec{J}x\overline{B} - (\frac{\mu}{k_1})\overline{V} - \rho\overline{g} \tag{2.2}$$

The heat equation

$$\rho C_p \frac{dT}{dt} = k_f \nabla^2 T + Q(T - T_o) \tag{2.3}$$

The concentration equation

$$\frac{dC}{dt} = D_m \nabla^2 C - kc(C - C_o) + \frac{D_m K_T}{T_m} \nabla^2 T \tag{2.4}$$

The equation of state is

$$\rho - \rho_0 = -\beta_T (T - T_o) - \beta_C (C - C_o) \tag{2.5}$$

The constitutive equation for the extra stress tensor S is (*)

$$S = (\mu + (\mu_o - \mu_\infty)\left(1 - \Gamma \dot{\gamma}\right)^{-1} \dot{\gamma} \tag{2.6}$$

And $\dot{\gamma}$ is defined by

$$\dot{\gamma} = \sqrt{0.5 \sum_i \sum_j \dot{\gamma}_{ij} \dot{\gamma}_{ji}} = \sqrt{0.5\Pi} \tag{2.7}$$

By considering $\mu_\infty = 0$ and $\Gamma \dot{\gamma}$ in the constitutive equation (2.6) ,so we can write

$$S = -\mu_o \left(1 - \Gamma \dot{\gamma}\right)^{-1} \dot{\gamma} \tag{2.8}$$

In which equation (2.8) reduces to a Newtonian fluid in case Γ =0.

The components of the extra stress tensor are

$$\tau_{xx} = 2\mu_o (1 + \Gamma \dot{\gamma}) \frac{\partial u}{\partial x}$$

$$\tau_{xy} = \tau_{yx} = \mu_o (1 + \Gamma \dot{\gamma})(\frac{\partial u}{\partial x} + \frac{\partial v}{\partial y})$$

$$\tau_{yy} = 2\mu_o (1 + \Gamma \dot{\gamma}) \frac{\partial v}{\partial y} \tag{2.9}$$

$$\tau_{xz} = \tau_{zx} = \tau_{yz} = \tau_{zy} = \tau_{zz} = 0$$

We consider the peristaltic transport of an incompressible electrically conducting Williamson fluid through a porous medium in a three dimensional symmetric flexible channel of width 2a taking Hall currents into account .The flow are considered in the direction of x-axis and z-axis is taken normal to the flow. A sinusoidal wave of amplitude b propagates along the channel walls with constant speed c along the direction of the x-axis. A string uniform magnetic field with magnetic flux density B =0 (B0Sinα, 0) is applied normal to the channel .The induced magnetic field is negligible assuming the magnetic Reynolds number (Rm) to be small. Also we assume that there is no applied or polarization voltage so that the total electric field E=0.The geometry of the wall surface is described by

$$H(x,t) = \pm a \pm bCos(\frac{2\pi}{\lambda}(X - ct)) \tag{2.10}$$

The generalized Ohm's law can be written as

$$\vec{J} = \sigma(\overline{E} + \vec{V}x\vec{B} - \beta\overline{J}x\vec{B}) \tag{2.11}$$

Where $\beta = \frac{1}{n_e e}$ is the Hall factor

Equation (2.10) can be solved in J to give rise to the Lorentz force vector i9n the form

$$\vec{J}x\vec{B} = \frac{\sigma B_o Sin(\alpha)}{1 + m^2 Sin^2(\alpha)}(mUSin(\alpha) - W)\vec{i} + (U + mWSin(\alpha)) \tag{2.12}$$

Where U and W are the velocity components along X and Z directions respectively. $m = \omega_e \tau_e$ is the Hall parameter.

The equation (2.1) in two-dimensional can be written as

$$\frac{\partial U}{\partial x} + \frac{\partial W}{\alpha z} = 0 \tag{2.13}$$

$$\rho(U\frac{\partial U}{\partial X} + W\frac{\partial U}{\partial Z}) = -\frac{\partial p}{\partial X} + \frac{\partial \tau_{xx}}{\partial X} + \frac{\partial \tau_{xz}}{\partial Z} - \frac{\sigma B_o Sin(\alpha)}{1 + m^2 Sin^2(\alpha)}(mUSin(\alpha) - W) - (\frac{\mu}{k1})u + \beta_T g(T - T_o) + \beta_C g(C - C_o) \tag{2.14}$$

$$\rho(U\frac{\partial W}{\partial X} + W\frac{\partial W}{\partial Z}) = -\frac{\partial p}{\partial Z} + \frac{\partial \tau_{xx}}{\partial X} + \frac{\partial \tau_{zz}}{\partial Z} - \frac{\sigma B_o Sin(\alpha)}{1 + m^2 Sin^2(\alpha)}(U + mWSin(\alpha)) - (\frac{\mu}{k1})W \tag{2.15}$$

$$\rho C_P(U\frac{\partial T}{\partial X} + W\frac{\partial T}{\partial Z}) = k_f \frac{\partial^2 T}{\partial Z^2} - Q_H(T - T_0) \tag{2.16}$$

$$(U\frac{\partial C}{\partial X} + W\frac{\partial C}{\partial Z}) = D_m \frac{\partial^2 C}{\partial Z^2} - k_c(C - C_0) + \frac{D_m K_T}{T_m}\frac{\partial^2 T}{\partial Z^2} \tag{2.17}$$

$\tau_{xx}, \tau_{xz}, \tau_{zz}$ are the components of the extra stress tensor equations (2.9)

$$\frac{\tau_{xx}}{\rho} = \frac{2\mu_0}{\rho}[\frac{\partial U}{\partial X} + \Gamma\frac{\partial U}{\partial X}\{(\frac{\partial U}{\partial X})^2 + \frac{1}{2}(\frac{\partial U}{\partial Z} + \frac{\partial W}{\partial X}) + (\frac{\partial W}{\partial Z})\}^1/2] \tag{2.18}$$

$$\frac{\tau_{xz}}{\rho} = \frac{\mu_0}{\rho}[1 + \Gamma\frac{\partial U}{\partial X}\{(\frac{\partial U}{\partial X})^2 + \frac{1}{2}(\frac{\partial U}{\partial Z} + \frac{\partial W}{\partial X}) + (\frac{\partial W}{\partial Z})\}^1/2\}\} \tag{2.19}$$

$$\frac{\tau_{zz}}{\rho} = \frac{2\mu_0}{\rho}[\frac{\partial W}{\partial Z} + \Gamma\frac{\partial W}{\partial Z}\{(\frac{\partial U}{\partial X})^2 + \frac{1}{2}(\frac{\partial U}{\partial Z} + \frac{\partial W}{\partial X}) + (\frac{\partial W}{\partial Z})\}^1/2] \tag{2.20}$$

We define the similarity variables as

$$x^{\bullet}=\frac{X}{\lambda}, z^{\bullet}=\frac{Z}{d1}, u^{\bullet}=\frac{U}{c}, w^{\bullet}=\frac{W}{c}, t^{\bullet}=\frac{c}{\lambda}t, \gamma^{\bullet}=\dot{\gamma}\frac{a}{c}, p^{\bullet}=\frac{a^{2}p}{\mu c\lambda},$$
$$\psi^{\bullet}=\frac{\psi}{ca}, h=\frac{H}{a}, \theta^{\bullet}=\frac{T-T_{o}}{T_{1}-T_{o}}, \phi^{\bullet}=\frac{C-C_{o}}{C_{1}-C_{o}} \tag{2.21}$$

Substituting 2.8-2.11 in equations (2.14-2.16) and using (2.20), the non-dimensional equations in terms of stream function ψ are

$$\delta\,\mathrm{Re}[(\frac{\partial\psi}{\partial x}\frac{\partial}{\partial z}-\frac{\partial\psi}{\partial z}\frac{\partial}{\partial x})\frac{\partial\psi}{\partial z}]=-\frac{\partial p}{\partial x}+2\delta^{2}\frac{\partial}{\partial x}[(1+We\dot{\gamma})\frac{\partial^{2}\psi}{\partial x\partial z}]+$$
$$\frac{\partial}{\partial x}[(1+We\dot{\gamma})(\frac{\partial^{2}\psi}{\partial z^{2}}-\delta^{2}\frac{\partial^{2}\psi}{\partial x^{2}}]+\delta[\frac{mM^{2}Sin(\alpha)}{1+m^{2}Sin^{2}(\alpha)}]\frac{\partial^{2}\psi}{\partial z^{2}}- \tag{2.22}$$
$$[\frac{M^{2}Sin(\alpha)}{1+m^{2}Sin^{2}(\alpha)}+D^{-1}][\frac{\partial\psi}{\partial z}+1]+G(\theta+N\phi]=0$$

$$-\delta^{3}\,\mathrm{Re}[(\frac{\partial\psi}{\partial z}\frac{\partial}{\partial x}-\frac{\partial\psi}{\partial x}\frac{\partial}{\partial z})\frac{\partial\psi}{\partial x}]=-\frac{\partial p}{\partial z}+\delta^{2}\frac{\partial}{\partial x}[(1+We\dot{\gamma})(\frac{\partial^{2}\psi}{\partial z^{2}}-\delta^{2}\frac{\partial^{2}\psi}{\partial x^{2}}]]$$
$$-2\delta^{2}\frac{\partial}{\partial z}[(1+We\dot{\gamma})\frac{\partial^{2}\psi}{\partial x\partial z}]-\delta[\frac{mM^{2}Sin(\alpha)}{1+m^{2}Sin^{2}(\alpha)}][\frac{\partial\psi}{\partial z}+1]$$
$$-\delta^{2}[\frac{mM^{2}Sin(\alpha)}{1+m^{2}Sin^{2}(\alpha)}+\frac{1}{\delta D}]\frac{\partial\psi}{\partial x}=0$$

(2.23)

$$\delta\,\mathrm{Re}[(\frac{\partial\psi}{\partial z}\frac{\partial\theta}{\partial z}-\frac{\partial\psi}{\partial x}\frac{\partial\theta}{\partial x})]=\frac{1}{\mathrm{Pr}}[\delta^{2}\frac{\partial^{2}\theta}{\partial x^{2}}+(1+\frac{4Rd}{3})\frac{\partial^{2}\theta}{\partial z^{2}}]-Q\theta \tag{2.24}$$

$$\delta\,\mathrm{Re}[(\frac{\partial\psi}{\partial z}\frac{\partial C}{\partial x}-\frac{\partial\psi}{\partial x}\frac{\partial C}{\partial z})]=\frac{1}{Sc}[\delta^{2}\frac{\partial^{2}C}{\partial x^{2}}+\frac{\partial^{2}C}{\partial z^{2}}]-\gamma C+Sr[\delta^{2}\frac{\partial^{2}\theta}{\partial x^{2}}+\frac{\partial^{2}\theta}{\partial z^{2}}]$$

Where

$$\dot{\gamma}=(4\delta^{2}(\frac{\partial^{2}\psi}{\partial x\partial z})^{2}+(\frac{\partial^{2}\psi}{\partial z^{2}}-\delta^{2}\frac{\partial^{2}\psi}{\partial x^{2}})^{2})^{1/2}, \mathrm{Re}=\frac{\rho c d}{\mu}\ \textit{is the Reynolds number},$$

$$M^{2}=\frac{\sigma B_{o}^{2}a}{\mu^{2}}\ \textit{is the magnetic Reynolds Number}, D=\frac{k_{1}}{a^{2}}\ \textit{is the permeabiulity parameter},$$

$$Sr=\frac{\rho D_{m}K_{T}(T_{1}-T_{o})}{\mu T_{m}(C_{1}-C_{o})}\ \textit{is the Soret parameter}, \mathrm{Pr}=\frac{\mu C_{P}}{k_{f}}\ \textit{is the prandtl number},$$

$$Sc=\frac{\mu}{\rho D_{m}}\ \textit{is the Schmidt number}, We=\frac{\Gamma c}{a}\ \textit{is the Weisseberg number},$$

$$Q=\frac{Q_{H}d^{2}}{k_{f}}\ \textit{is the Heat source parameter}, G=\frac{\beta_{T}g(T_{1}-T_{o})\lambda^{3}}{ca}\ \textit{is the Grashof number}$$

$N=\dfrac{\beta_{C}(C_{1}-C_{o})}{\beta_{T}(T_{1}-T_{0})}$ *is the Buoyancy ratio*, $\gamma=\dfrac{k_{c}\lambda^{2}}{ca}$ is the chemical reaction parameter, $\delta=\dfrac{d}{\lambda}$

Under the assumptions of long wavelength (δ <<1) and low Reynolds number, we obtain

$$0=-\frac{\partial p}{\partial x}+\frac{\partial}{\partial z}((1+We\frac{\partial^2\psi}{\partial z^2})\partial^2\psi)-(\frac{M^2 Sin(\alpha)}{1+m^2 Sin^2(\alpha)}+D^{-1})(\frac{\partial\psi}{\partial z}+1)+G(\theta+NC) \tag{2.25}$$

$$0=-\frac{\partial p}{\partial y} \tag{2.26}$$

$$0=\frac{1}{\Pr}(1+\frac{4Rd}{3})\frac{\partial^2\theta}{\partial z^2}-Q\theta \tag{2.27}$$

$$0=\frac{1}{Sc}\frac{\partial^2 C}{\partial z^2}-\gamma C+Sr\frac{\partial^2\theta}{\partial z^2} \tag{2.28}$$

Equation (2.26) shows that p # p(z), and we can write equation(2.25) in the form

$$0=\frac{\partial^2}{\partial z^2}((1+We\frac{\partial^2\psi}{\partial z^2})\partial^2\psi)-(\frac{M^2 Sin(\alpha)}{1+m^2 Sin^2(\alpha)}+D^{-1})(\psi)+\frac{G}{\mathrm{Re}}G(\frac{d\theta}{dz}+N\frac{dC}{dz}) \tag{2.29}$$

The non-dimensional boundary conditions in the wave frame are given by

$$\psi=0,\frac{\partial^2\psi}{\partial z^2}=0,\theta=0,C=0\ on\ \ z=0 \tag{2.30}$$

$$\psi=q,\frac{\partial\psi}{\partial z}=-1,\theta=1,C=1\ on\ \ z=h \tag{2.31}$$

Where $h(z)=1+\varepsilon Cos(2\pi x),\varepsilon=\frac{b}{a}$ the amplitude ratio and q is is the non-dimensional time mean flow rate in the wave frame. It is related to the dimensionless time mean flow rate Q in the laboratory frame through the relation

$$Q=q+1$$

The non-dimensional pressure drop Δp per wave length is

$$\Delta p=\int_0^1\frac{dp}{dx}dx \tag{2.32}$$

To solve the equations (2.27, 2.28, 2.29) with the boundary conditions (2.30&21.31) we adopt a perturbation technique with We<<1and we take

$$\psi=\psi_o+We\psi_1+We^2\psi_2+\ldots\ldots\ldots\ldots\ldots\ldots\ldots\ldots \tag{2.33}$$

$$q=q_o+We\,q_1+We^2q_2+\ldots\ldots\ldots\ldots\ldots\ldots \tag{2.34}$$

$$\frac{dp}{dx}=\frac{dp_o}{dx}+We\frac{dp_1}{dx}+We^2\frac{dp_2}{dx}+\ldots\ldots\ldots\ldots\ldots\ldots \tag{2.35}$$

$$\theta=\theta_0+We\theta_1+We^2\theta_2+\ldots\ldots\ldots\ldots\ldots\ldots \tag{2.36}$$

$$C = C_0 + WeC_1 + We^2 C_2 + \ldots\ldots\ldots\ldots\ldots \qquad (2.37)$$

Substituting (2.33-2.37) in equations (2.27, 2.28, 2.29) and equating the coefficients of We, up to the first order and neglecting powers of order 2 and higher, we get

Zeroth order

$$0 = -[\frac{\partial^4 \psi_0}{\partial z^4} - (\frac{M^2 Sin(\alpha)}{1+m^2 Sin^2(\alpha)} + D^{-1})\frac{\partial^2 \psi_0}{\partial z^2} + G(\frac{\partial \theta_o}{\partial z} + N\frac{\partial C_o}{\partial z}) \qquad (2.38)$$

$$0 = (1+\frac{4Rd}{3})\frac{1}{\Pr}\frac{\partial^2 \theta_0}{\partial z^2} - Q\theta_0) \qquad (2.39)$$

$$0 = \frac{1}{Sc}\frac{\partial^2 C_0}{\partial z^2} - \lambda C_0 + Sr\frac{\partial^2 \theta_0}{\partial z^2} \qquad (2.40)$$

The corresponding boundary conditions are

$$\psi_0 = 0, \frac{\partial^2 \psi_0}{\partial z^2} = 0, \theta_o = 0, C_o = 0 \quad on \quad z = 0 \qquad (2.41)$$

$$\psi_0 = qo, \frac{\partial^2 \psi_0}{\partial z^2} = -1,, \theta_o = 1, C_o = 1 \quad on \quad z = h \qquad (2.42)$$

The first order equations are

$$0 = -[\frac{\partial^4 \psi_1}{\partial z^4} - (\frac{M^2 Sin(\alpha)}{1+m^2 Sin^2(\alpha)} + D^{-1})\frac{\partial^2 \psi_1}{\partial z^2} + \frac{\partial^2}{\partial z^2}(\frac{\partial^2 \psi_o}{\partial z^2})^2 + G(\frac{\partial \theta_1}{\partial z} + N\frac{\partial C_{1o}}{\partial z}) \qquad (2.43)$$

$$0 = (1+\frac{4Rd}{3})\frac{1}{\Pr}\frac{\partial^2 \theta_1}{\partial z^2} - Q\theta_1 \qquad (2.44)$$

$$0 = \frac{1}{Sc}\frac{\partial^2 C_1}{\partial z^2} - \lambda C_1 + Sr\frac{\partial^2 \theta_1}{\partial z^2} \qquad (2.45)$$

The co0rresponding first order boundary conditions

$$\psi_1 = 0, \frac{\partial^2 \psi_1}{\partial z^2} = 0, \theta_1 = 0, C_1 = 0 \quad on \quad z = 0 \qquad (2.46)$$

$$\psi_1 = q_1, \frac{\partial^2 \psi_1}{\partial z^2} = 0,, \theta_1 = 0, C_1 = 0 \quad on \quad z = h \qquad (2.47)$$

Solving the equations (2.38-2.40) subject to the conditions (2.41-2.42) the zeroth order solutions are

$$\theta_o = \frac{Sinh(\beta_1 z)}{Sinh(\beta_1 h)} \qquad (2.48)$$

$$C_0 = \frac{Sinh(\beta_2 z)}{Sinh(\beta_2 h)} + \frac{A_1}{\beta_1^2 - \beta_2^2}(\frac{Sinh(\beta_2 z)}{Sinh(\beta_2 h)}Sinh(\beta_1 h) - Sinh(\beta_1 z) \qquad (2.49)$$

$$\psi_0 = A_6 Sinh(M_1 z) + A_7 Sinh(M_1 z) + A_8 z + A_9 + A_4 Cosh(\beta_1 z) + A_5 Sinh(\beta_1 z)$$

(2.50)

The first order solutions are

$$\theta_1 = 0 \tag{2.51}$$

$$C_1 = 0$$

$$\psi_1 = A_{26}Cosh(M_1 z) + A_{27}Sinh(M_1 z) + A_{28}z + A_{29} + f_1(z)$$
$$f_1(z) = -A_{12}Cosh(2M_1 z) - A_{13}Cosh(2\beta_1 z) - A_{14}Cosh(2\beta_2 z) - A_{15}Sinh(2M_1 z) - A_{16}Cosh(M_2 z) - A_{17}Cosh(M_3 z) - A_{18}Cosh(M_4 z) - A_{19}Cosh(M_5 z) - A_{20}Sinh(M_2 z) - - A_{21}Sinh(M_3 z) - A_{22}Sinh(M_4 z) - A_{23}Sinh(M_5 z) - A_{24}Cosh(M_5 z) - A_{25}Cosh(M_4 z) \tag{2.52}$$

Where

$$\beta_1^2 = \frac{3QRd}{3+4Rd}, \beta_2^2 = Sc\,\gamma, A_1 = \frac{ScSr\,\beta_1^2}{Sinh(\beta_1 h)},\ A_2 = Gr\left(\frac{\beta_1}{Sinh(\beta_1 h)} - \frac{A_1\beta_1}{\beta_1^2 - \beta_2^2}\right)$$

$$A_3 = GrNr\left(\frac{\beta_2}{Sinh(\beta_2 h)} + \frac{A_2\beta_2 Sinh(\beta_1 h)}{(\beta_1^2 - \beta_2^2)Sinh(\beta_2 h)}\right),$$

$$A_4 = \frac{A_2}{\beta_1^2(\beta_1^2 - M_1^2)} \quad , \quad A_5 = \frac{A_3}{\beta_2^2(\beta_2^2 - M_1^2)}$$

$$A_6 = -\frac{A_4\beta_1^2}{M_1^2}, A_9 = \frac{A_4(\beta_1^2 - M_1^2)}{M_1^2},$$

$$A_{10} = A_4\beta_1^2 Cosh(\beta_1 h) + A_5\beta_2^2 Cosh(\beta_2 h) - 1$$

$$A_{11} = A_4 Cosh(\beta_1 h) + A_5 Cosh(\beta_2 h),\ A_7 = -\frac{A_6 M_1^2 Cosh(M_1 h) + A_{10}}{M_1^2 Sinh(M_1 h)},$$

$$A_8 = \frac{[q_0 - A_6 Cosh(M_1 h) - A_9 - A_{11} - A_7 Sinh(M_1 h)]}{h}, A_{12} = \frac{(A_6^2 + A_7^2)M_1^2}{6},$$

$$A_{13} = \frac{(A_4^2)\beta_1^6}{2\beta_1^2(4\beta_1^2 - M_1^2)},\ A_{14} = \frac{(A_5^2)\beta_2^6}{2\beta_2^2(4\beta_2^2 - M_1^2)},\ A_{15} = \frac{(A_6 A_7)M_1^2}{3},$$

$$A_{16} = \frac{A_4 A_6 \beta_1^2 M_1^2 M_2^2}{M_2^2(M_2^2 - M_1^2)}, A_{17} = \frac{A_4 A_6 \beta_1^2 M_1^2 M_3^2}{M_3^2(M_3^2 - M_1^2)},$$

$$A_{18} = \frac{A_5 A_6 \beta_{21}^2 M_1^2 M_4^2}{M_4^2(M_4^2 - M_1^2)}, A_{19} = \frac{A_5 A_6 \beta_1^2 M_1^2 M_5^2}{M_5^2(M_5^2 - M_1^2)},$$

$$A_{20} = \frac{A_4 A_7 \beta_1^2 M_1^2 M_2^2}{M_2^2(M_2^2 - M_1^2)},\ A_{21} = \frac{A_4 A_7 \beta_1^2 M_1^2 M_3^2}{M_3^2(M_3^2 - M_1^2)},$$

$$A_{22} = \frac{A_5 A_7 \beta_2^2 M_1^2 M_4^2}{M_4^2(M_4^2 - M_1^2)}, A_{23} = \frac{A_5 A_7 \beta_2^2 M_1^2 M_5^2}{M_5^2(M_5^2 - M_1^2)},\ A_{24} = \frac{A_4 A_5 \beta_1^2 \beta_2^2 \beta_3^2}{\beta_3^2(\beta_3^2 - M_1^2)},$$

$$A_{25} = \frac{A_4 A_5 \beta_1^2 \beta_2^2 \beta_4^2}{\beta_4^2(\beta_4^2 - M_1^2)},\ \beta_3 = \frac{\beta_1 + \beta_2}{2}, \beta_4 = \frac{\beta_1 - \beta_2}{2}$$

$$M_2 = \frac{M_1+\beta_1}{2}, M_3 = \frac{M_1-\beta_1}{2},$$

$$M_4 = \frac{M_1+\beta_2}{2}, M_5 = \frac{M_1-\beta_2}{2},$$

$$B1 = -4A_{12}M_1^2 - 4A_{13}\beta_1^2 - 4A_{14}\beta_2^2 - A_{16}M_2^2 - A_{17}M_2^2 - A_{18}M_4^2 - A_{19}M_5^2 - A_{24}\beta_3^2 - A_{25}\beta_4^2$$

$$A_{26} = -\frac{B_1}{M_1^2}, f_1(h) = B_3, f_1^{'}(h) = B_4, A_{29} = -B_2 - A_{26},$$

$$A_{30} = q_1 + B_3 + hB_4 + A_{29} + A_{26}Cosh(M_1h) - M_1hA_{26}Sinh(M_1h),$$

$$A_{27} = \frac{A_{30}}{(Sinh(M_1h) - hCosh(M_1h))}, A_{28} = -B_4 - M_1A_{26}Sinh(M_1h) - M_1A_{27}Cosh(M_1h)$$

$$A_{31} = A_{26}M_1^4 + 2A_1M_1^3 - A_{27}M_1^3 - 2A_{22}M_1^2, A_{32} = A_{27}M_1^2 - A_{22}M_1^4 - A_{26}M_1^3 + 2A_6M_1^3,$$

$$A_{33} = 2A_4A_6M_1^2\beta_1^4 + 2A_5A_7M_1^4\beta_1^2 + 2A_5A_6M_1^2\beta_1^4 + 2A_5A_7M_1^2\beta_1^4 - A_{20}M_1^2M_2,$$

$$A_{34} = -A_{20}M_2^4 - A_{16}M_1^2M_2 + 2A_5A_6^2M_1^4\beta_1^2,$$

$$A_{35} = A_4A_6 - A_5A_7 + A_5A_6M_1^2\beta_1^4 - A_5A_7M_1^2\beta_1^4 - 2A_{21}M_3,$$

$$A_{36} = -A_{21}M_3^4 - A_5A_6M_1^4\beta_1^2 + A_4A_7M_1^3\beta_1^2 - A_{17}M_3,$$

$$A_{37} = -2A_{18}M_4, A_{38} = -A_{23}M_5^4 - 2A_{19}M_5, A_{39} = -2A_{23}M_5 - A_{19}M_5^4, A_{40} = 2A_4\beta_1^3,$$

$$A_{41} = 2A_5\beta_1^3, A_{42} = -A_{24}\beta_3^4, A_{43} = -A_{25}\beta_3^4, A_{44} = -16A_{12}M_1^4 + 0.5A_6M_1^6 + 0.5A_7M_1^6 + 2M_1^3A_{15},$$

$$A_{45} = A_6A_7M_1^6 - 2M_1^3A_{12}, A_{46} = -16A_{13}M_1^4 + A_4^2\beta_1^6 + A_5^2\beta_1^6 + A_4A_7\beta_1^6,$$

$$A_{47} = -16\beta_2^4A_{14}, A_{48} = 2A_{13}M_1^2, A_{49} = 2\beta_2M_1^2A_{14}, A_{50} = A_{25}\beta_4M_1^2,$$

$$A_{51} = A_6^2M_1^6 + A_7^2M_1^6 - A_5^2\beta_1^6 + A_4^2\beta_1^6$$

$$\begin{aligned}
B_{44} = \frac{dp_0}{dx} = &[A_6M_1^2(Ch(M_1h)-1) + A_7M_1^2Sh(M_1h) + A_4\beta_1^2(Ch(\beta_1h)-1) + A_5\beta_1^2Sh(\beta_1h) \\
&- M_1^2(A_6(Ch(M_1h)-1) + A_7Sh(M_1h) + A_8h + A_4(Ch(\beta_1h)-1) + A_5Sh(\beta_1h) + G(\frac{(Ch(\beta_1h)-1)}{\beta_1Sh(\beta_1h)} \\
&+ Nr(\frac{(Ch(\beta_2h)-1)}{\beta_2Sh(\beta_2h)} + \frac{A_1}{\beta_1^2-\beta_2^2}(\frac{(Ch(\beta_2h)-1)}{\beta_2Sh(\beta_2h)}Sh(\beta_1h) - \frac{(Ch(\beta_1h)-1)}{\beta_1})) - Q]/hB_{44} = [A_6M_1^2(Ch(M_1h)-1) + A_7M_1^2Sh(M_1h) + A_4\beta_1^2(Ch(\beta_1h)-1) + A_5\beta_1^2Sh(\beta_1h) \\
&- M_1^2(A_6(Ch(M_1h)-1) + A_7Sh(M_1h) + A_8h + A_4(Ch(\beta_1h)-1) + A_5Sh(\beta_1h) + G(\frac{(Ch(\beta_1h)-1)}{\beta_1Sh(\beta_1h)} \\
&+ Nr(\frac{(Ch(\beta_2h)-1)}{\beta_2Sh(\beta_2h)} + \frac{A_1}{\beta_1^2-\beta_2^2}(\frac{(Ch(\beta_2h)-1)}{\beta_2Sh(\beta_2h)}Sh(\beta_1h) - \frac{(Ch(\beta_1h)-1)}{\beta_1})) - Q]/h[A_6M_1^2(Ch(M_1h)-1) + A_7M_1^2Sh(M_1h) + A_4\beta_1^2(Ch(\beta_1h)-1) + A_5\beta_1^2Sh(\beta_1h) \\
&- M_1^2(A_6(Ch(M_1h)-1) + A_7Sh(M_1h) + A_8h + A_4(Ch(\beta_1h)-1) + A_5Sh(\beta_1h) + G(\frac{(Ch(\beta_1h)-1)}{\beta_1Sh(\beta_1h)} \\
&+ Nr(\frac{(Ch(\beta_2h)-1)}{\beta_2Sh(\beta_2h)} + \frac{A_1}{\beta_1^2-\beta_2^2}(\frac{(Ch(\beta_2h)-1)}{\beta_2Sh(\beta_2h)}Sh(\beta_1h) - \frac{(Ch(\beta_1h)-1)}{\beta_1})) - Q]/h
\end{aligned}$$

$$\begin{aligned}
B_{55} = \frac{dp_1}{dx} = &[\frac{A_{31}}{M_1}Sh(M_1h) + \frac{A_{32}}{M_1}(Ch(M_1h)-1) + \frac{A_{33}}{M_2}Sh(M_2h) + \frac{A_{37}}{M_4}(Ch(M_4h)-1) \\
&+ \frac{A_{38}}{M_5}(Ch(M_5h)-1) + \frac{A_{39}}{M_5}Sh(M_5h) + \frac{A_{40}}{\beta_1}(Ch(\beta_1h)-1) + \frac{A_{41}}{\beta_1}Sh(\beta_1h) + \frac{A_{42}}{\beta_3}Sh(\beta_3h) \\
&+ \frac{A_{43}}{\beta_3}(Ch(\beta_3h)-1) + \frac{A_{44}}{2M_1}Sh(2M_1h) + \frac{A_{45}}{2M_1}(Ch(2M_1h)-1) + \frac{A_{46}}{2\beta_1}Sh(2\beta_1h) + \frac{A_{47}}{2\beta_2}Sh(2\beta_2h) \\
&+ \frac{A_{48}}{2\beta_1}(Ch(2\beta_1h)-1) + \frac{A_{49}}{2\beta_2}(Ch(2\beta_2h)-1) + \frac{A_{50}}{\beta_4}(Ch(\beta_4h)-1) + A_{51}h - \overline{Q_1}]/h
\end{aligned}$$

RESULTS AND DISCUSSION:

In this section, we have presented a set of figures that describe qualitatively the effects of various parameters of interest on the flow characteristics, like axial velocity(u),temperature (θ),concentration(C), pressure drop(Δp),frictional force,(F), rate of heat and mass transfer(Nu&Sh).

The axial velocity(u) is depicted in figures 2-13 for different variations of G,M,m, Da, Rd, α,Sc,γ,Sr,We,ξ ,Pr and ε.

An increase in Grashof number (G) and magnetic parameter (M) increases the central region and reduces ion the region adjacent to the wall y=1(figs.2&3).Fig.4 represents u with Hall parameter (m).From the profiles we find that the axial velocity reduces in the central region and enhances it in the region abutting the wall y=1.

Fig.5 shows the variation of u with buoyancy ratio (Nr).It can be seen from the profiles that when the molecular buoyancy force dominates over the thermal force, the velocity enhances when the buoyancy forces are in the same directions and for the forces acting in opposite directions, it reduces in the entire flow region.

Fig.6 depicts u with radiation parameter (Rd).From the profiles we find that higher the thermal radiation, u reduces in the central region and enhances is the region adjacent to the abutting y=1.

In fig.7 wee analyse the axial velocity with heat source parameter(α).In the presence of heat generating source, the velocity enhances in the central region and reduces in the region adjacent to the wall y=1 while in the presence of heat absorption, heat is depreciated in the central region and enhances in the region adjacent to y=1.

Lesser the molecular diffusivity (Sc), smaller the velocity in the central region and increases in the region adjacent to the wall y=1(fig.8).

Fig.9 illustrates u with chemical reaction parameter(γ).It can be seen from the profiles that the velocity increases in the degenerating chemical reaction case, while in the generating case, u increases in the region(0,0.6) and reduces in the region(0.6,1.0).

Higher the thermo-diffusion (Sr) smaller u in the central region and larger u in the region abutting y=1(fig.10).

Fig.11&14 shows the variation of u with different values of Wessenberg number (We) and inclination (ξ) of the inclined magnetic field. From the graphs. We find that the axial velocity reduces in the central region and increases in the region adjacent to y=1.

Fig.12 represents u with amplitude ε of the wavy boundary. From the profiles we find that the axial velocity reduces/enhances with increase in amplitude ξ of the wavy boundary.

Fig.13 shows the variation of u with Prandtl number(Pr).From the figure we find that lesser the thermal diffusivity the magnitude of u increases in the central region of the channel and decrease s in the region adjacent to y=1.

Figs.15-19represent the variation of temperature (θ) with different values of Rd,α,Pr,ξ and ε.We follow the convention that the non-dimensional temperature (θ) is positive/negative according as the actual temperature(T) is greater/lesser than the temperature (T2) on the wavy wall y=1.Fig.15 represents θ with heat source parameter(α).From the profiles we find that the actual temperature reduces with increase in the strength of the heat generating source and enhances with that of heat absorbing source in the entire region except in the central region(0.5,0.8) where it reduces w2ith α>0 and α<0.From fig.16 &18find that higher the thermal radiation/lesser the thermal diffusivity(Pr) smaller the actual temperature in the entire flow region. An increase in the inclination (ξ) of the magnetic field smaller the actual temperature in the entire flow region except at y=0.6, where it enhances (fig.19) .The actual temperature experiences a depreciation with increasing values of amplitude (ε) of the wavy wall (fig.17).

Figs.20-27 show the variation of concentration (C) with different values of Rd,α, Sc, Sr,γ,ξ,ε and Pr. We follow the convention that the non-dimensional concentration (C) is positive/negative according as the actual concentration(C) is greater/lesser than the concentration (C2) on the wavy wall y=1.Higher the thermal radiation larger the actual concentration except at y=0.6 where it reduces (fig.21). With reference to heat source parameter (α), we find that the actual concentration enhances in the central region of the channel and reduces in the vicinity of the right wavy wall with increase in the heat generation, while a reversed effect is noticed in the case of heat absorption (fig.20).Lesser the molecular diffusivity smaller the actual concentration in the flow region (fig.23). The actual concentration enhances in both the degenerating and generating chemical reaction casers except at y=0.6 where it depreciates(fig.24).With reference to Soret parameter(Sr) we find that higher the thermo-diffusion effects larger the actual concentration except at y=0.6 where it depreciates(fig.25).An increase in the amplitude ε,it reduces except at y=0.6 where it reduces(figs.26).From fig.22 we observe that lesser the thermal diffusivity larger the actual concentration except at y=0.6 where it depreciates.Fig.27 shows the variation of C with inclination (ξ) of the magnetic field. From the profiles we find that an increase in ξ reduces the actual concentration in the entire flow region except in the region (0.5, 0.8) where it enhances withξ.

The pressure rise per wave length (Δp) against flow rate $\overline{Q}$ for different values of Grashof number(G), Magnetic parameter(M), Darcy parameter(Da), Hall parameter(m), Schmidt number(Sc),Soret parameter(Sr), chemical reaction parameter(γ)., radiation parameter(Rd), heat source parameter(α), Weissenberg number(We), amplitude(ε) of the wavy wall, inclination angle of the magnetic field(ξ), Prandtl number(Pr) are illustrated in Figs.28-40.Equation(2.32) involve the integration of $\frac{dp}{sx}$.This integral is not solvable analytically so it is computed numerically by using "Mathematica". It is obvious from figs.28-40 that the in the pumping region (Δp>0), the pumping rate increases with increase in Grashof number G and magnetic parameter (M)(figs.28&29).An increase in Darcy parameter(Da) or hall parameter(m) reduces the pumping rate(figs.30&31) .With reference to buoyancy ratio(Nr),we find that when the molecular buoyancy force dominates over the thermal force ,the pumping rate increases when the buoyancy forces are in the same direction and the forces acting in opposite directions, it reduces(fig.32). An increase in radiation parameter (Rd≤ 1.5) the pumping rate reduces while for still higher Rd≥ 3.5, it enhances (fig.33). For the pumping rate (Δp>0) and in co-pumping region ((Δp<0), the pumping rate decreases with increasing values of both α>0 and α<0(fig.34).The pumping rate reduces with Sc and increases with Soret parameter (Sr) (figs.35&36).With respect to chemical reaction parameter (γ),we find that the pumping rate reduces in the degenerating chemical reaction case and enhances in the generating case. Also an increase in amplitude ε of the wavy wall or inclination (ξ) of the magnetic field enhances the pumping rate in the pumping region(Δp>0)(figs.38&39).With reference to Prandtl number (Pr<1.71) we find that in the pumping region(Δp>0) ,the pumping rate increases, while for higher Pr>3.71,the pumping rate reduces in the co-pumping region(fig.40).

The frictional force(F) against flow rate $\overline{Q}$ for different values of Grashof number(G), Magnetic parameter(M), Darcy parameter(Da), Hall parameter(m), Schmidt number(Sc), Soret parameter(Sr),chemical reaction parameter(γ).,radiation parameter(Rd), heat source parameter(α), Weissenberg number(We), Amplitude(ε) of the wavy wall, inclination angle of the magnetic field(ξ), Prandtl number(Pr) are illustrated in Figs.41-53.We find that the magnitude of the frictional force increases with increase in Grashof number(G), magnetic parameter(M),Hall parameter(m)(figs.41-43) and reduces with that of Darcy parameter(Da)(fig.44).With reference to buoyancy ratio(Nr) we find that when the molecular buoyancy force dominates over the thermal buoyancy force the frictional force increases irrespective of the directions of the buoyancy forces(fig.45). Higher the thermal radiation (Rd)/ lesser the molecular diffusivity (Sc) smaller the force (figs.46&48). With respect to heat source parameter (α), we find that the magnitude of F reduces with increase in the strength of he heat generating/absorbing source higher the thermo-diffusion effects larger the magnitude of F (fig.47). The magnitude of F reduces in the degenerating chemical reaction case and increases in generating case (fig.50). An increase in the amplitude (ε)/inclination (ξ) of the magnetic field larger |F|(figs.51&52).With reference to Prandtl number(Pr),we find that F is negative for Pr≤1.71 and is positive for higher Pr≥3.71,In total |F| reduces with increasing values of Pr(fig.53).

The rate of heat transfer (Nu) on the wall. (y=1) is exhibited in figs.55-58 for different parametric variations. From the graphs we find that higher the thermal radiation (Rd) / lesser the thermal diffusivity (Pr) larger the rate of heat transfer on the wall (figs.54&57). The variation of Nu with heat source parameter (α) shows that The Nusselt number increases with increase in α>0 and reduces with the strength of the heat absorbing source (fig.55). Higher the amplitude (ε)/ inclination (ξ) of the magnetic field, smaller the rate of heat transfer at the wall (figs.56&58).

The rate of mass transfer (Sherwood number) at the wall y=1 is shown in figs.59-66 for different variations of the parameters. Higher the thermal radiation/thermo-diffusion effects, larger the rate of mass transfer (figs.61&62). An increase in heat generating source parameter (α≤4)larger Sh and for still α≥6,smaller Sh at the wall(fig.63). Lesser the moleculer diffusivity (Sc≤0.66) larger Sh and still lowering of the diffusivity (Sc≥1.3) smaller Sh on the wall (fig.59). The rate of mass of mass transfer enhances in both degenerating/generating chemical reaction cases (fig.60). Sh reduces with increase inn the amplitude (ε) and enhances with the inclination (ξ) of the magnetic field (figs64&66). Lesser the thermal diffusivity (Pr≤1.71) larger Sh and for still higher Pr≥3.71, Sh reduces at the wavy wall y=1 (fig.65).

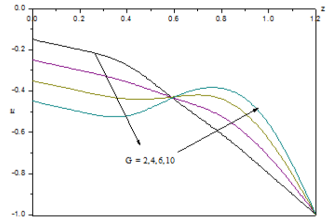

Fig. 2 : Variation of u with G
M=1, m=0.5, Nr=1, Rd=0.5, α=2, Sc=1.3, γ=0.5, Sr=0.5, We=0, ε=0.1, Pr=0.71, $\xi=\pi/2$

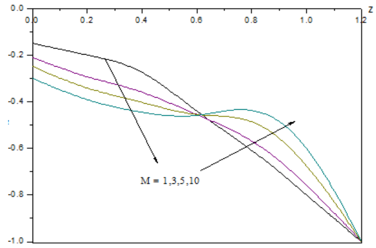

Fig. 3 : Variation of u with M
G=2, m=0.5, Nr=1, Rd=0.5, α=2, Sc=1.3, γ=0.5, Sr=0.5, We=0, ε=0.1, Pr=0.71, $\xi=\pi/2$

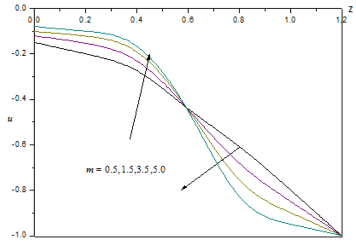

Fig. 4 : Variation of u with m
G=2, M=1, Nr=1, Rd=0.5, α=2, Sc=1.3, γ=0.5, Sr=0.5, We=0, ε=0.1, Pr=0.71, $\xi=\pi/2$

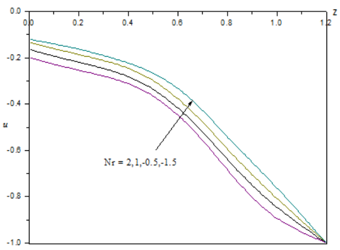

Fig. 5 : Variation of u with Nr
G=2, M=1, m=0.5, Rd=0.5, α=2, Sc=1.3, γ=0.5, Sr=0.5, We=0, ε=0.1, Pr=0.71, $\xi=\pi/2$

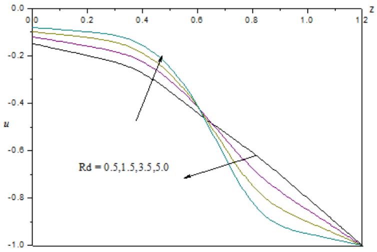

Fig. 6 : Variation of u with Rd
G=2, M=1, m=0.5, Nr=1, α=2, Sc=1.3, γ=0.5, Sr=0.5, We=0, ε=0.1, Pr=0.71, $\xi=\pi/2$

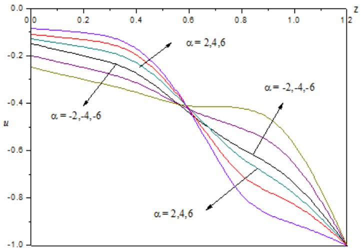

Fig. 7 : Variation of u with α
G=2, M=1, m=0.5, Nr=1, Rd=0.5, Sc=1.3, γ=0.5, Sr=0.5, We=0, ε=0.1, Pr=0.71, $\xi=\pi/2$

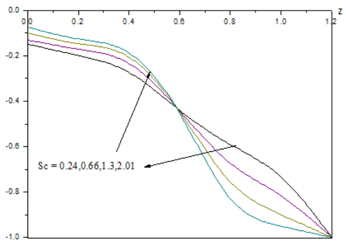

Fig. 8 : Variation of u with Sc
G=2, M=1, m=0.5, Nr=1, Rd=0.5, α=2, γ=0.5, Sr=0.5, We=0, ε=0.1, Pr=0.71, $\xi=\pi/2$

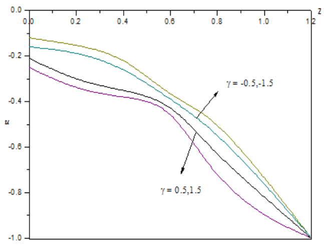

Fig. 9 : Variation of u with γ
G=2, M=1, m=0.5, Nr=1, Rd=0.5, α=2, Sc=1.3, Sr=0.5, We=0, ε=0.1, Pr=0.71, $\xi=\pi/2$

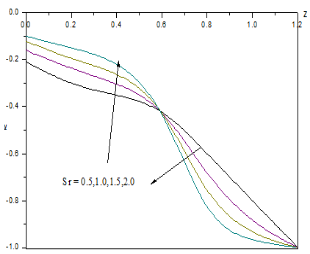

Fig. 10 : Variation of u with Sr
G=2, M=1, m=0.5, Nr=1, Rd=0.5, α=2, Sc=1.3, γ=0.5, We=0, ε=0.1, Pr=0.71, $\xi=\pi/2$

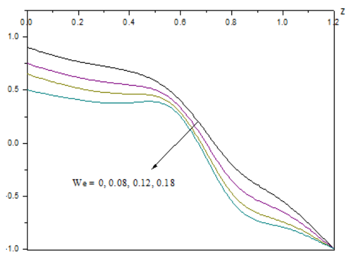

Fig. 11 : Variation of u with We
G=2, M=1, m=0.5, Nr=1, Rd=0.5, α=2, Sc=1.3, γ=0.5, Sr=0.5, ε=0.1, Pr=0.71, $\xi=\pi/2$

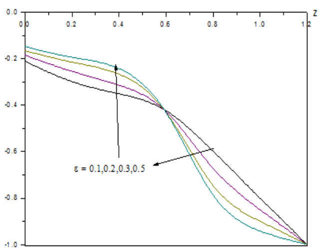

Fig. 12: Variation of u with ε
G=2, M=1, m=0.5, Nr=1, Rd=0.5, α=2, Sc=1.3, γ=0.5, Sr=0.5, We=0, Pr=0.71, $\xi=\pi/2$

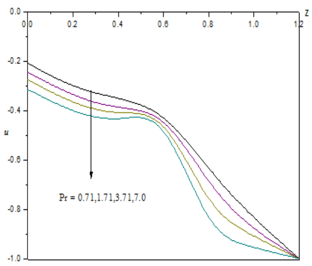

Fig. 13: Variation of u with Pr
G=2, M=1, m=0.5, Nr=1, Rd=0.5, α=2, Sc=1.3, γ=0.5, Sr=0.5, We=0, ε=0.1, $\xi=\pi/2$

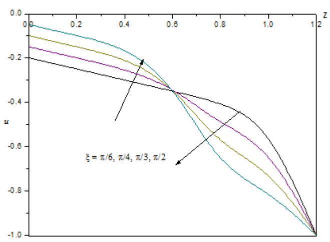

Fig. 14: Variation of u with ξ
G=2, M=1, m=0.5, Nr=1, Rd=0.5, α=2, Sc=1.3, γ=0.5, Sr=0.5, We=0, ε=0.1, Pr=0.71

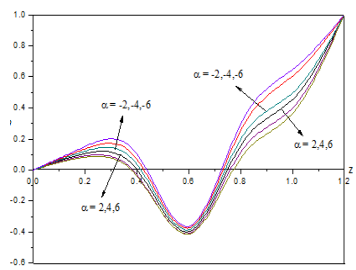

Fig. 15 : Variation of θ with α
Rd=0.5, ε=0.1, Pr=0.71, $\xi=\pi/2$

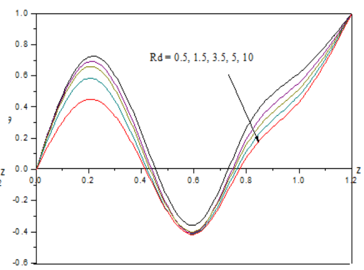

Fig. 16: Variation of θ with Rd
α=2, ε=0.1, Pr=0.71, $\xi=\pi/2$

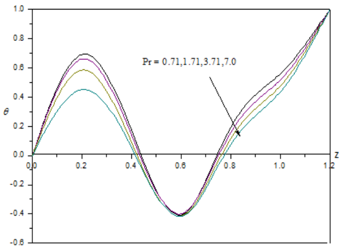

Fig. 17: Variation of θ with Pr
α=2, Rd=0.5, ε=0.1, $\xi=\pi/2$

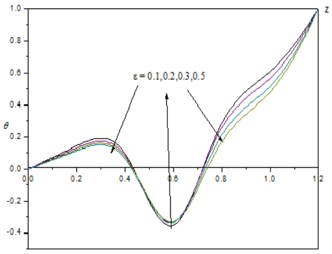

Fig. 18: Variation of θ with ε
α=2, Rd=0.5, Pr=0.71, $\xi=\pi/2$

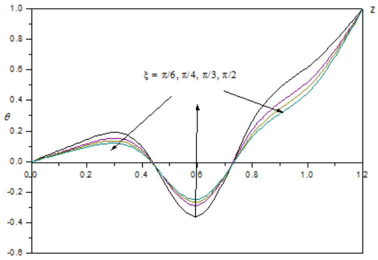

Fig. 19: Variation of θ with ξ
α=2, Rd=0.5, ε=0.1, Pr=0.71

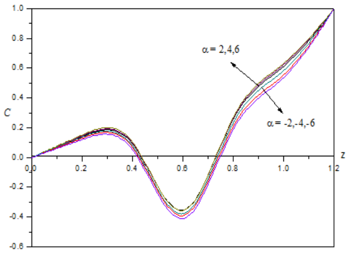

Fig. 20: Variation of C with α
Rd=0.5, Pr=0.71, Sc=1.3, γ=0.5,
Sr=0.5, ε=0.1, $\xi=\pi/2$

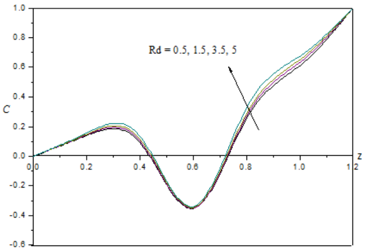

Fig. 21: Variation of C with Rd
α=2, Pr=0.71, Sc=1.3, γ=0.5,
Sr=0.5, ε=0.1, $\xi=\pi/2$

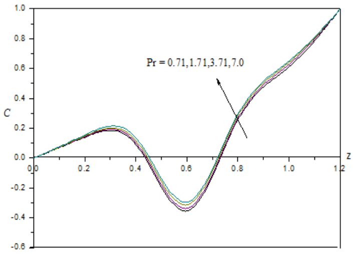

Fig. 22: Variation of C with Pr
α=2, Rd=0.5, Sc=1.3, γ=0.5,
Sr=0.5, ε=0.1, $\xi=\pi/2$

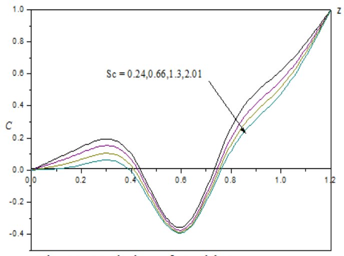

Fig. 23: Variation of C with Sc
α=2, Rd=0.5, Pr=0.71, γ=0.5,
Sr=0.5, ε=0.1, $\xi=\pi/2$

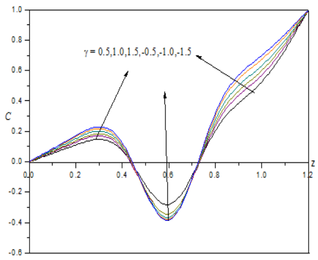

Fig. 24: Variation of C with γ
α=2, Rd=0.5, Pr=0.71, Sc=1.3,
Sr=0.5, ε=0.1, $\xi=\pi/2$

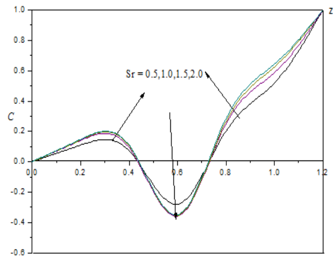

Fig. 25: Variation of C with Sr
α=2, Rd=0.5, Pr=0.71, Sc=1.3,
γ=0.5, ε=0.1, $\xi=\pi/2$

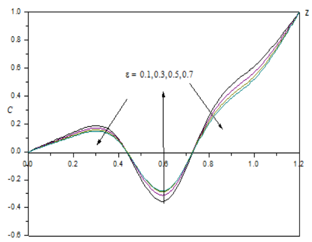

Fig. 26: Variation of C with ε
α=2, Rd=0.5, Pr=0.71, Sc=1.3,
γ=0.5, Sr=0.5, $\xi=\pi/2$

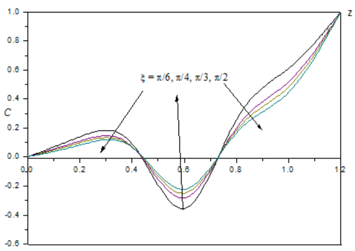

Fig. 27: Variation of C with ξ
α=2, Rd=0.5, Pr=0.71, Sc=1.3, γ=0.5,
Sr=0.5, ε=0.1

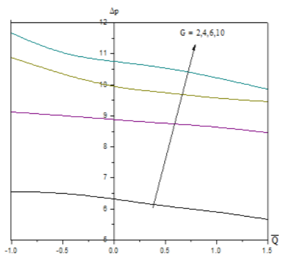

Fig. 28: Variation of Δp with G
M=1, m=0.5, Da=1, Nr=1, Rd=0.5, α=2, Sc=1.3,
Sr=0.5, γ=0.5, ε=0.1, $\xi=\pi/2$, Pr=0.71

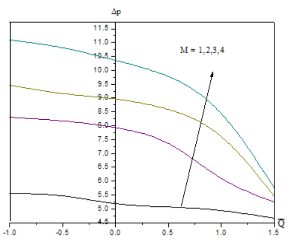

Fig. 29: Variation of Δp with M
G=2, m=0.5, Da=1, Nr=1, Rd=0.5, α=2, Sc=1.3,
Sr=0.5, γ=0.5, ε=0.1, $\xi=\pi/2$, Pr=0.71

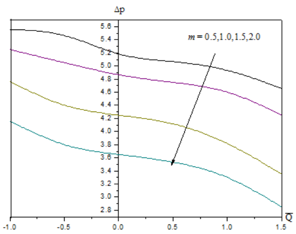

Fig. 30: Variation of Δp with m
G=2, M=1, Da=1, Nr=1, Rd=0.5, α=2, Sc=1.3,
Sr=0.5, γ=0.5, ε=0.1, $\xi=\pi/2$, Pr=0.71

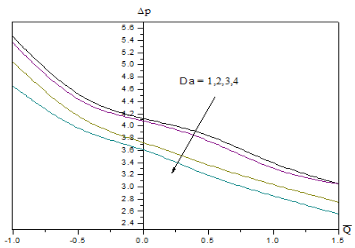

Fig. 31: Variation of Δp with Da
G=2, M=1, m=0.5, Nr=1, Rd=0.5, α=2, Sc=1.3,
Sr=0.5, γ=0.5, ε=0.1, $\xi=\pi/2$, Pr=0.71

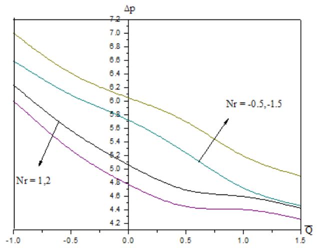

Fig. 32: Variation of Δp with Nr
G=2, M=1, m=0.5, Da=1, Rd=0.5, α=2, Sc=1.3, Sr=0.5, γ=0.5, ε=0.1, ξ=π/2, Pr=0.71

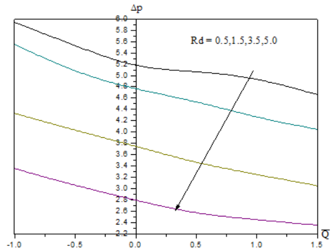

Fig. 33: Variation of Δp with Rd
G=2, M=1, m=0.5, Da=1, Nr=1, α=2, Sc=1.3, Sr=0.5, γ=0.5, ε=0.1, ξ=π/2, Pr=0.71

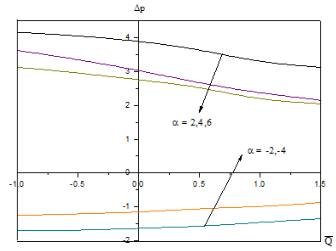

Fig. 34: Variation of Δp with α
G=2, M=1, m=0.5, Da=1, Nr=1, Rd=0.5, Sc=1.3, Sr=0.5, γ=0.5, ε=0.1, ξ=π/2, Pr=0.71

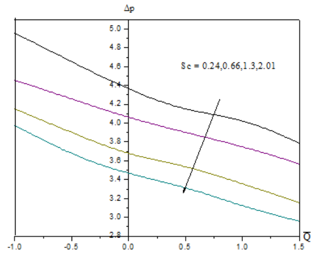

Fig. 35: Variation of Δp with Sc
G=2, M=1, m=0.5, Da=1, Nr=1, Rd=0.5, α=2, Sr=0.5, γ=0.5, ε=0.1, ξ=π/2, Pr=0.71

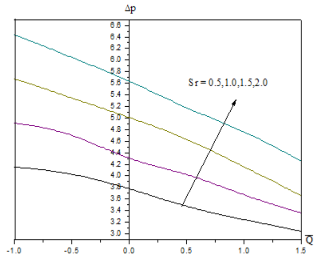

Fig. 36: Variation of Δp with Sr
G=2, M=1, m=0.5, Da=1, Nr=1, Rd=0.5, α=2, Sc=1.3, γ=0.5, ε=0.1, ξ=π/2, Pr=0.71

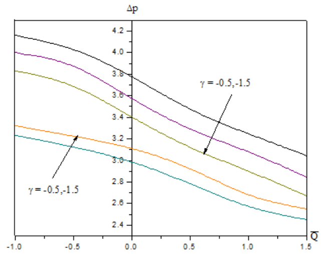

Fig. 37: Variation of Δp with γ
G=2, M=1, m=0.5, Da=1, Nr=1, Rd=0.5, α=2, Sc=1.3, Sr=0.5, ε=0.1, ξ=π/2, Pr=0.71

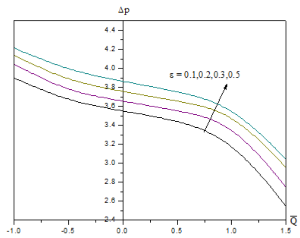

Fig. 38: Variation of Δp with ε
G=2, M=1, m=0.5, Da=1, Nr=1, Rd=0.5, α=2, Sc=1.3, Sr=0.5, γ=0.5, ξ=π/2, Pr=0.71

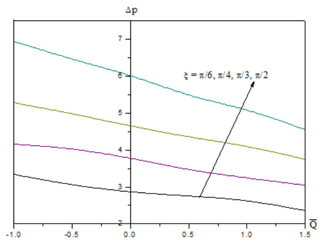

Fig. 39: Variation of Δp with ξ
G=2, M=1, m=0.5, Da=1, Nr=1, Rd=0.5, α=2, Sc=1.3, Sr=0.5, γ=0.5, ε=0.1, Pr=0.71

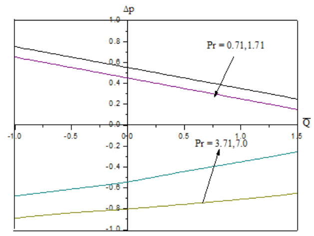

Fig. 40: Variation of Δp with Pr
G=2, M=1, m=0.5, Da=1, Nr=1, Rd=0.5, α=2, Sc=1.3, Sr=0.5, γ=0.5, ε=0.1, ξ=π/2

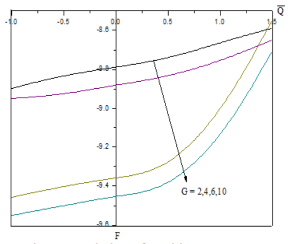

Fig. 41: Variation of *F* with G
M=1, m=0.5, Da=1, Nr=1, Rd=0.5, α=2, Sc=1.3, Sr=0.5, γ=0.5, ε=0.1, ξ=π/2, Pr=0.71

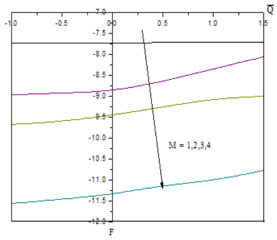

Fig. 42: Variation of *F* with M
G=2, m=0.5, Da=1, Nr=1, Rd=0.5, α=2, Sc=1.3, Sr=0.5, γ=0.5, ε=0.1, ξ=π/2, Pr=0.71

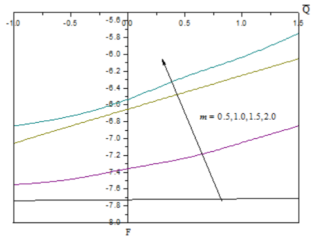

Fig. 43: Variation of *F* with m
G=2, M=1, Da=1, Nr=1, Rd=0.5, α=2, Sc=1.3, Sr=0.5, γ=0.5, ε=0.1, ξ=π/2, Pr=0.71

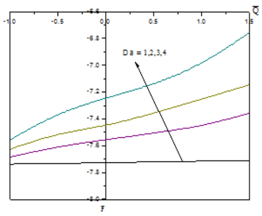

Fig. 44: Variation of *F* with Da
G=2, M=1, m=0.5, Nr=1, Rd=0.5, α=2, Sc=1.3, Sr=0.5, γ=0.5, ε=0.1, ξ=π/2, Pr=0.71

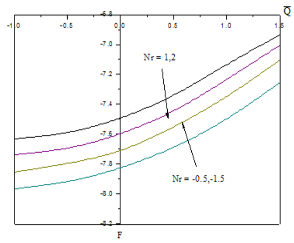

Fig. 45: Variation of *F* with Nr
G=2, M=1, m=0.5, Da=1, Rd=0.5, α=2, Sc=1.3, Sr=0.5, γ=0.5, ε=0.1, ξ=π/2, Pr=0.71

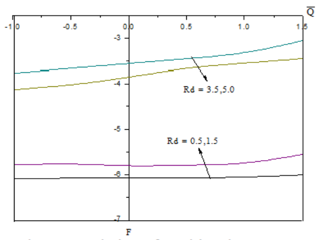

Fig. 46: Variation of *F* with Rd
G=2, M=1, m=0.5, Da=1, Nr=1, α=2, Sc=1.3, Sr=0.5, γ=0.5, ε=0.1, ξ=π/2, Pr=0.71

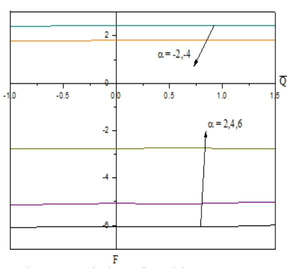

Fig. 47: Variation of F with α
$G=2, M=1, m=0.5, Da=1, Nr=1, Rd=0.5, Sc=1.3, Sr=0.5, \gamma=0.5, \varepsilon=0.1, \xi=\pi/2, Pr=0.71$

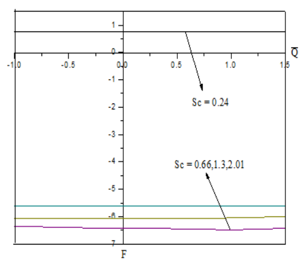

Fig. 48: Variation of F with Sc
$G=2, M=1, m=0.5, Da=1, Nr=1, Rd=0.5, \alpha=2, Sr=0.5, \gamma=0.5, \varepsilon=0.1, \xi=\pi/2, Pr=0.71$

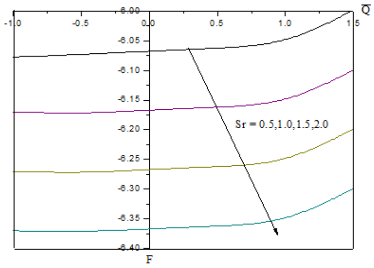

Fig. 49: Variation of F with Sr
$G=2, M=1, m=0.5, Da=1, Nr=1, Rd=0.5, \alpha=2, Sc=1.3, \gamma=0.5, \varepsilon=0.1, \xi=\pi/2, Pr=0.71$

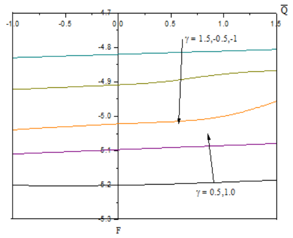

Fig. 50: Variation of F with γ
$G=2, M=1, m=0.5, Da=1, Nr=1, Rd=0.5, \alpha=2, Sc=1.3, Sr=0.5, \varepsilon=0.1, \xi=\pi/2, Pr=0.71$

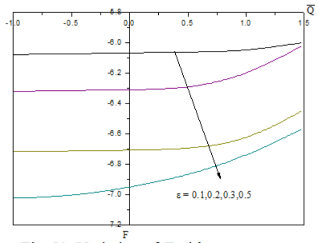

Fig. 51: Variation of F with ε
$G=2, M=1, m=0.5, Da=1, Nr=1, Rd=0.5, \alpha=2, Sc=1.3, Sr=0.5, \gamma=0.5, \xi=\pi/2, Pr=0.71$

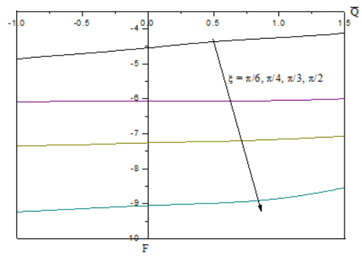

Fig. 52: Variation of F with ξ
$G=2, M=1, m=0.5, Da=1, Nr=1, Rd=0.5, \alpha=2, Sc=1.3, Sr=0.5, \gamma=0.5, \varepsilon=0.1, Pr=0.71$

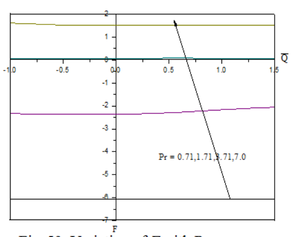

Fig. 53: Variation of F with Pr
$G=2, M=1, m=0.5, Da=1, Nr=1, Rd=0.5, \alpha=2, Sc=1.3, Sr=0.5, \gamma=0.5, \varepsilon=0.1, \xi=\pi/2$

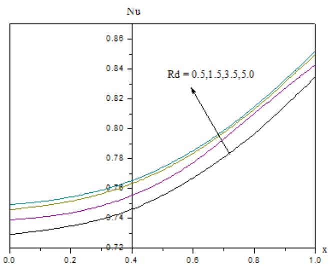

Fig. 54: Variation of Nu with Rd
$\alpha=2, \varepsilon=0.1, Pr=0.71, \xi=\pi/2$

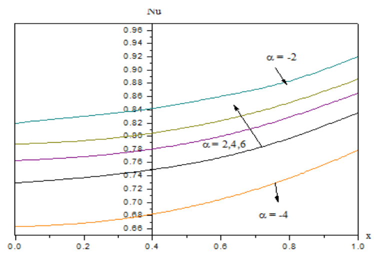

Fig. 55: Variation of Nu with α
$Rd=0.5, \varepsilon=0.1, Pr=0.71, \xi=\pi/2$

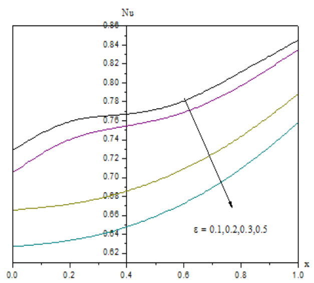

Fig. 56: Variation of Nu with ε
$Rd=0.5, \alpha=2, Pr=0.71, \xi=\pi/2$

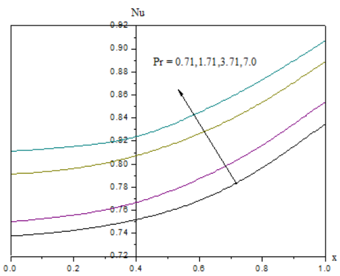

Fig. 57: Variation of Nu with Pr
$Rd=0.5, \alpha=2, \varepsilon=0.1, \xi=\pi/2$

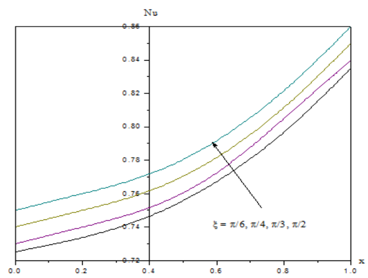

Fig. 58: Variation of Nu with ξ
$Rd=0.5, \alpha=2, \varepsilon=0.1, Pr=0.71$

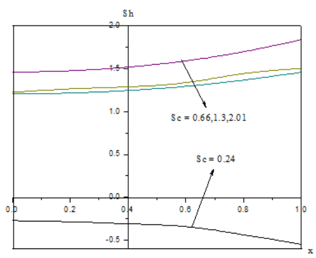

Fig. 59: Variation of Sh with Sc
$\gamma=0.5, Sr=0.5, Rd=0.5, \alpha=2, \varepsilon=0.1, Pr=0.71, \xi=\pi/2$

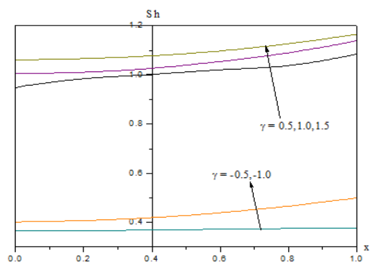

Fig. 60: Variation of Sh with γ
$Sc=1.3, Sr=0.5, Rd=0.5, \alpha=2, \varepsilon=0.1, Pr=0.71, \xi=\pi/2$

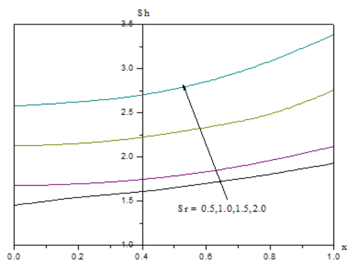

Fig. 61: Variation of Sh with Sr
$Sc=1.3, \gamma=0.5, Rd=0.5, \alpha=2, \varepsilon=0.1, Pr=0.71, \xi=\pi/2$

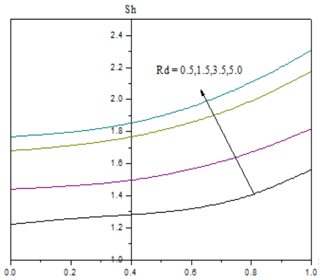

Fig. 62: Variation of *Sh* with Rd
Sc=1.3, γ=0.5, Sr=0.5, α=2,
ε=0.1, Pr=0.71, ξ=π/2

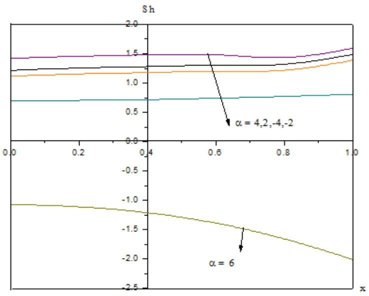

Fig. 63: Variation of *Sh* with α
Sc=1.3, γ=0.5, Sr=0.5, Rd=0.5,
ε=0.1, Pr=0.71, ξ=π/2

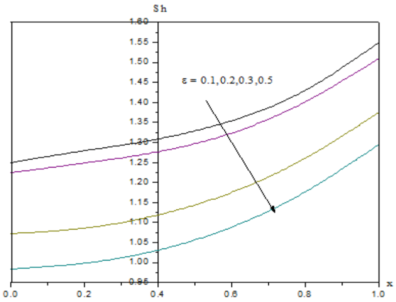

Fig. 64: Variation of *Sh* with ε
Sc=1.3, γ=0.5, Sr=0.5, Rd=0.5,
α=2, Pr=0.71, ξ=π/2

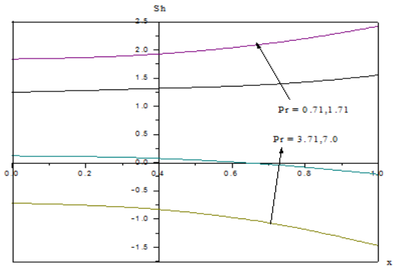

Fig. 65: Variation of *Sh* with Pr
Sc=1.3, γ=0.5, Sr=0.5, Rd=0.5,
α=2, ε=0.1, ξ=π/2

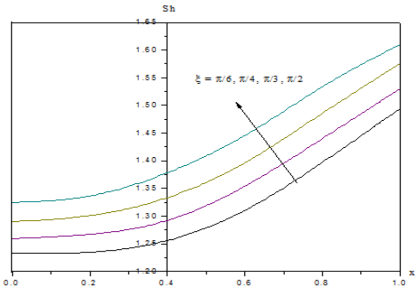

Fig. 66: Variation of *Sh* with ξ
Sc=1.3, γ=0.5, Sr=0.5, Rd=0.5,
α=2, ε=0.1, Pr=0.71

CONCLUSIONS

This paper addresses the thermal radiation heat sources, Hall effects, inclination of the magnetic field on the peristaltic motion of Williamson fluid. The main observations have been summarized as follows:

- An increase in Grashof number (G)/magnetic parameter (M) reduces u in the central region and enhances in the vicinity of y=1.The pressure drop (Δp) increases while the frictional force (F) decreases with G.
- An increase in Hall parameter (m)/Radiation parameter (Rd) enhances u in the central region and reduces in the vicinity of y=1.The pressure drop (Δp) decreases while the frictional force (F) increases with m. The temperature reduces and the concentration enhances with increase in Rd.
- An increase in Soret parameter (Sr) enhances u in the central region and reduces in the vicinity of y=1.The pressure drop (Δp) increases while the frictional force decreases with Rd. The Sherwood number (Sh) increases with Sr.
- An increase in heat source parameter(α>0) enhances u in the central region and reduces in the region adjacent to y=1,while reversed effect is observed with α<0.An increase in α>0,reduces the temperature ,enhances the concentration, pressure drop, frictional force, Nusselt and Sherwood number, while reversed effect is noticed in their behaviour with α<0.
- An increase in the inclination (ξ) of the magnetic field increases u in the central region and reduces in the vicinity of y=1.The temperature, concentration, frictional force reduces while the pressure drop, Nusselt and Sherwood number enhance with increase inξ.
- An increase in Weissenberg number we reduces the velocity u in the entire flow region.

REFERENCES

[1] Akram, S. Nadeem, S and Hanif, M: Numerical and analytical treatment on peristaltic flow of Williamson fluid in the occurrence of induced magnetic field, *J. Magn. Magn. Mater.* **346** (2013) 142–151.

[2] Akram, S: Effects of nanofluid on peristaltic flow of a Carreau fluid model in an inclined magnetic field, *Heat Transfer-Asian Res.* **43** (2013) 368–383.

[3] B´eg, O.A Rashidi, M.M, B´eg T. A and Asadi, M: Homotopy analysis of transient magneto-bio-fluid dynamics of micropolar squeeze film in a porous medium: A model for magneto-bio-rheological lubrication, *J. Mech. Med. Biol.* **12** (2012) 1250051, 21 pp.

[4] Dapra and Scarpi, G., Perturbation solution for pulsatile flow of a non-Newtonian Williamson fluid in a rock fracture. International Journal of Rock Mechanics and Mining Sciences, 44, 271 (2007).

[5] Ellahi R., The effects of MHD and temperature-dependent viscosity on the flow of non-Newtonian nanofluid in a pipe: Analytical solutions, *Appl. Math. Model.* **37** (2013) 1451–1457.

[6] Ellahi, R, Aziz, S. and Zeeshan, A: Non-Newtonian nanofluid flow through a porous medium between two coaxial cylinders with heat transfer and variable viscosity, *J. Porous Media* **16** (2013) 205–216.

[7] Ellahi, R. Raza Mand, Vafai, K: Series solutions of non-Newtonian nanofluids with Reynolds' model and Vogel's model by means of the homotopy analysis method, *Math. Comput. Model.* **55** (2012) 1876–1891.

[8] El-Sayed, M.F, Eldabe, N.T.M, Ghaly, A.Y and. Sayed, H.M: Magnetohydrodynamic peristaltic flow of Bingham non-Newtonian fluid in eccentric annuli with slip velocity and temperature jump conditions, *J. Mech.* **29** (2013) 493–506.

[9] Eytan.O and Elad, D: Analysis of intra-uterine fluid motion induced by uterine contractions, *Bull. Math. Biol.* **61** (1999) 221–238.

[10] Fetecau, C, Athar, M and Fetecau,C: Unsteady flow of a generalized Maxwell fluid with fractional derivative due to a constantly accelerating plate, *Comput. Math. Appl.* **57** (2009) 596–603.

[11] Humaira Yasmin,Hayat,TNaif Alotaibi and Huijun Gao:Convective heat and mass transfer analysis on peristaltic flow of Williamson fluid with Hall effects and Joule heating., International Journal of Biomathematics,V.7(5),pp.1-27,(2014)

[12] Jyothi B, Koteswara Rao P, Slip effects on MHD peristaltic transport of a Williamson fluid through a porous medium in a symmetric channel, Journal of Mathematical and Computational Science, 3(5), 2013, pp 1306-1324.

[13] Khalid AL-QAissy,Ahmed M.Abdulhadi:Effect of magnetic field on peristaltic flow of Williamson fluid in a symmetric channel.,IOSR Journal of Mathematics, V.13(1),pp.30-39(2017)

[14] Lew H. S., Fung Y. C. and Lowenstein C. B., Peristaltic carrying and mixing of chyme, *J. Biomech.* **4** (1971) 297–315.

[15] Lyubimov, D. V. and Perminov, A. V., Motion of a thin oblique layer of a pseudo-plastic fluid. Journal of Engineering Physics and Thermophysics, 75, No. 4, 920 (2002).

[16] Mekheimer Kh. S., Abdelmaboud Y. and Abdellateef A. I., Peristaltic transport through eccentric cylinders: Mathematical model, *Appl. Bionics Biomech.* **10** (2013) 19–27.

[17] Misra J. C. and Maiti S., Peristaltic transport of rheological fluid: Model for movement of food bolus through esophagus, *Appl. Math. Mech.* **33** (2012) 315–332.

[18] Nadeem S., Maraj E. and Akbar N. S., Investigation of peristaltic flow of Williamson nanofluid in a curved channel with compliant walls, *Appl. Nanosci.* **4** (2014) 511–521.

[19] Naheeda Iftikhar, Abdul Rehman and Muhammad Najam Khan:Features of convective heat and mass transfer on MHD peristaltic movement of Williamson fluid with the presence of Joule heating.,IOP Conf.Sereies: Material Science and Engineering 414(2018)doi.102010 doi:10.1088/1757-899x/414/0/012010

[20] Navaneeswara Reddy S, Viswanatha Reddy G, Slip effects on peristaltic motion of a Williamson fluid through a porous medium in a planar channel, Asian Journal of Current Engineering and Maths, 2, 2013, pp 53-58.

[21] Noreen S. and Qasim M., Peristaltic flow of MHD Eyring–Powell fluid in a channel, *European Phys. J. Plus* **128** (2013) 91–101.

[22] Rashidi M. M., Ali M., Mehr N. F. and Nazari F., Parametric analysis and optimization of entropy generation in unsteady swarm optimization algorithm, *Energy* **55** (2013) 497–510.

[23] Rashidi M. M., Chamkha A. J. and Keimanesh M., Application of multi-step differential transform method on flow of a second-grade fluid over a stretching or shrinking sheet, *Amer. J. Comput. Math.* **6** (2011) 119–128.

[24] Rashidi M. M., Hayat T., Erfani E., Pour S. A. M. and Hendi A. A., Simultaneous effects of partial slip and thermal diffusion and diffusion-thermo on steady MHD convective flow due to a rotating disk, *Commun. Nonlinear Sci. Numer. Simulat.* **16** (2011) 4303–4317.

[25] Ravikumar S., Peristaltic flow of a couple stress fluid through magnetic field at low Reynolds number in a flexible channel under an oscillatory flux, *Int. J. Appl. Math. Mech.* **9** (2013) 1–14.

[26] Sarada,K and Shankar,B:Effect of partial slip and convective boundary condition on MHd mixed convection flow of Williamson fluid over an exponentially stretching sheet in the presence of joule heating.,Global journal of pure and Applioed Mathemqatics,V,13(9),pp.5965-5975(2017)

[27] Sheikholeslami M., Bandpy M. G., Ellahi R., Hassan M. and Soleimani S., Effects of MHD on Cu-water nanofluid flow and heat transfer by means of CVFEM, *J. Magn. Magn. Mater.* **349** (2014) 188–200.

[28] Srivastava L. M. and Srivastava V. P., Peristaltic transport of a power law fluid: Applications to the *ductus efferentes* of the reproductive tract, *Rheol. Acta* **27** (1988) 428–433.

[29] Strohmer H., Obruca A., Rander K. M. and Feichtinger W., Relationship of the individual uterine size and the endometrial thickness in stimulated cycles, *Fertil. Steril.* **61** (1994) 972–975.

[30] Sulochana,P:Combined effects on the peristaltic flow of Williamson fluid through a porous medium in a symmetric channel,asian journal of current engineering and maths,V.15,pp.94-103(2016)

[31] Tripathi D., Ali N., Hayat T., Chaube M. K. and Hendi A. A., Peristaltic flow of MHD Jeffrey fluid through finite length cylindrical tube, *Appl. Math. Mech.* **32** (2011) 1231–1244.

[32] Vajravelu K, Sreenadh S, Rajinikanth K, Changhoon Lee, Peristaltic transport of a Williamson fluid in asymmetric channels with permeable walls, Nonlinear Analysis: Real World Applications, 13(6), 2012, pp 2804-2822.

[33] Veerakrishna,M and Swarnalatha,B: Heat and mass transfer on the peristaltic flow of an incompressible electrically conducting Williamson fluid through a porous medium in a symmetric channel with Hall current effects and inclined magnetic field., International Journal of Scientific and Engineering research,V.6,No.9,pp.941-957,(2015)

[34] Veerakrishna,M and Swarnalatha,B:Convective heat and mass transfer on MHD peristaltic flow of Williamson fluid with the effect of inclined magnetic field., International conference on condensed Matter and Applied Physics(ICC 2015)AIP Conf Proc.1728,020461-1-020461-8;doi:10.1063/1,4946512

[35] Williamson, R. V., The flow of pseudo-plastic materials. Industrial & Engineering Chemistry Research, 21, No. 11, 1108 (1929).